



Towards a CAD-based automatic procedure for patient specific cutting guides to assist sternal osteotomies in pectus arcuatum surgical correction

Monica Carfagni^a, Flavio Facchini^b, Rocco Furferi^{a,*}, Marco Ghionzoli^b, Lapo Governi^a, Antonio Messineo^b, Francesca Uccheddu^a, Yary Volpe^a

^a Department of Industrial Engineering, University of Florence, Florence, Italy

^b Department of Pediatric Surgery, A. Meyer Children's University Hospital, Florence, Italy

ARTICLE INFO

Article history:

Received 2 November 2017

Received in revised form 22 December 2017

Accepted 1 January 2018

Available online 3 January 2018

Keywords:

Design for additive manufacturing

CAD

Medical imaging

Biomedical devices

ABSTRACT

Pectus Arcuatum, a rare congenital chest wall deformity, is characterized by the protrusion and early ossification of sternal angle thus configuring as a mixed form of excavatum and carinatum features. Surgical correction of pectus arcuatum always includes one or more horizontal sternal osteotomies, consisting in performing a V-shaped horizontal cutting of the sternum (resection prism) by means of an oscillating power saw. The angle between the saw and the sternal body in the V-shaped cut is determined according to the peculiarity of the specific sternal arch. The choice of the right angle, decided by the surgeon on the basis of her/his experience, is crucial for a successful intervention. The availability of a patient-specific surgical guide conveying the correct cutting angles can considerably improve the chances of success and, at the same time, reduce the intervention time. The present paper aims to propose a new CAD-based approach to design and produce custom-made surgical guides, manufactured by using additive manufacturing techniques, to assist the sternal osteotomy. Starting from CT images, the procedure allows to determine correct resection prism and to shape the surgical guide accordingly taking into account additive manufacturing capabilities. Virtually tested against three case studies the procedure demonstrated its effectiveness.

© 2018 Society for Computational Design and Engineering. Publishing Services by Elsevier. This is an open access article under the CC BY-NC-ND license (<http://creativecommons.org/licenses/by-nc-nd/4.0/>).

1. Introduction

Among all chest wall deformities, Pectus Excavatum represents the most common congenital malformation (Fokin, Steuerwald, Ahrens, & Allen, 2009). It is triggered by the abnormal growth of the connective tissue connecting the sternum and the adjacent ribs and it causes a depression of the sternal body. Pectus Carinatum is the second most encountered congenital chest wall deformity following Pectus Excavatum. It is characterized by a protrusion deformity of the chest wall (i.e. sternal and costal cartilage elevation) and it accounts for 5% of all chest wall deformities affecting 1 in 2500 live births (Martinez-Ferro, Fraire, & Bernard, 2008). A rarer category of deformations (less than 1% of all PC cases) is the Pectus

Arcuatum (PA), a congenital deformation where the patient manubrium sterni and superior costal cartilages results protruded. It includes mixed excavatum and carinatum features along a longitudinal or transversal axis causing a multiplanar curvature of the stern body (see Fig. 1 (Jeune, Carron, Beraud, & Loaec, 1954).

The psychological impact of such body malformations is often experienced among patients due to cosmetic appearance, especially among adolescent patients. This can significantly affect the daily quality of life and cause distress socially: causing difficulties in establishing friendship, relationships and, sometimes, can affect self-esteem and confidence.

Traditional approaches to the corrections of PA rely on surgical interventions that aim to increase the cardiorespiratory functions and restore kinetic and structural integrity while minimizing the risk of relapses or future deterioration of the chest wall (Kim et al., 2016). Treatment options were invasive initially, using skeletal correction techniques. Recently, more minimally invasive procedures are carried out to relocate the sternum to its normal position. Surgical correction of PA always includes one or more horizontal sternal osteotomies, resection of deformed rib cartilages and finally anterior chest wall stabilization.

Peer review under responsibility of Society for Computational Design and Engineering.

* Corresponding author.

E-mail addresses: monica.carfagni@unifi.it (M. Carfagni), flavio.facchini@meyer.it (F. Facchini), rocco.furferi@unifi.it (R. Furferi), marco.ghionzoli@meyer.it (M. Ghionzoli), lapo.governi@unifi.it (L. Governi), antonio.messineo@meyer.it (A. Messineo), francesca.uccheddu@unifi.it (F. Uccheddu), yary.volpe@unifi.it (Y. Volpe).

<https://doi.org/10.1016/j.jcde.2018.01.001>

2288-4300/© 2018 Society for Computational Design and Engineering. Publishing Services by Elsevier.

This is an open access article under the CC BY-NC-ND license (<http://creativecommons.org/licenses/by-nc-nd/4.0/>).

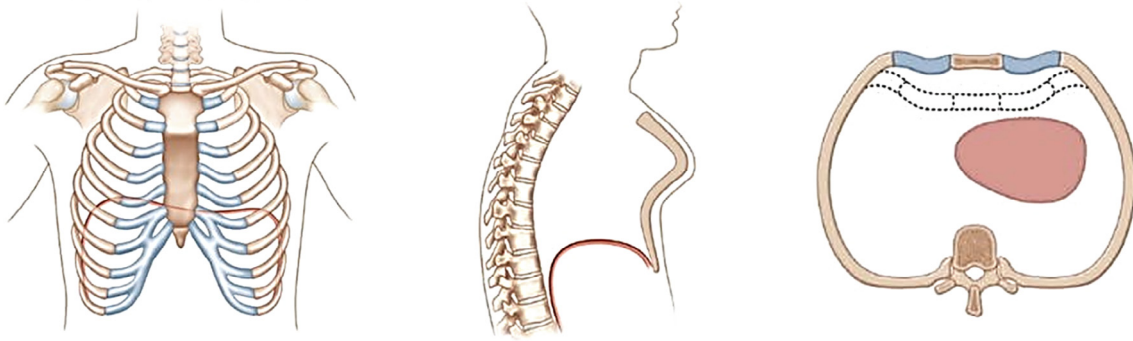


Fig. 1. Pectus Arcuatum (image from Jeune et al. (1954)).

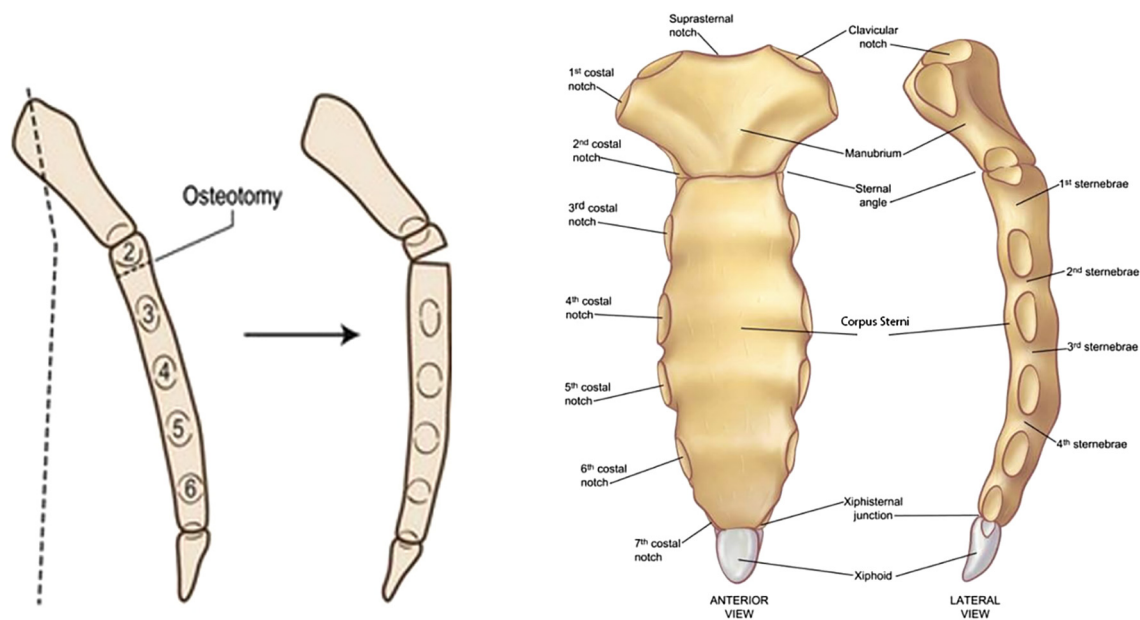


Fig. 2. Sternal osteotomy procedure (Fonkalsrud & Anselmo, 2004).

The sternal osteotomy procedure (see Fig. 2a) consists in performing a V-shaped horizontal cutting (actually defining a resection prism) by means of an oscillating power saw of the corpus sterni (from now on simply referred to as “sternum” see Fig. 2b) at the top of deformity by preserving the posterior cortex. The remodeling of the sternum is performed by downward pressuring at the top of deformity and then upward pulling of sternal body. This maneuver aims at breaking (if sternum is rigid) or bending of posterior cortex while preserving the posterior periosteum.

The angle between the saw and the sternal body in the V-shaped cut is determined according to the peculiarity of the specific sternal arch. The choice of the right angle, decided by the surgeon on the basis of her/his experience, is crucial to prevent overcorrections or undercorrections of the deformity, thus determining the success/unsuccess of the intervention.

Within such a scenario, the availability of a patient-specific surgical guide conveying the correct cutting angles could dramatically improve the chances of success and, at the same time, reduce the intervention time as well as the risk of infections. To this purpose, the combination of 3D reconstruction and Additive Manufacturing (AM) technology is ideally suited because of their unique ability to make optimized and customized devices even for complex geometries (Yao, Moon, & Bi, 2017). In fact, almost all medical interventions share techniques based on medical imaging (MI) and 3D reconstruction for diagnosis, education or intervention planning.

It is, therefore, straightforward to add 3D printing methods to this traditional workflow, when the complexity of the anatomy to be treated requires physical models to be managed by medical staff.

Some dedicated methods are referred to hip and knees prosthesis design (Goodfellow & O'Connor, 1978) as well as to maxillofacial sector (Farré-Guasch et al., 2015) and to personalized hand-wrist-arm orthosis design (Carfagni et al., 2017). Recently, a generalized integrated framework of semi-automatic surgical template design has been proposed in Chen, Xu, Yang, and Egger (2016). In detail, in such a work a general computer-aided design software was developed. Provided with an easy to use GUI, the proposed software can be useful for oral implantology and pedicle and iliosacral screw insertion. Inspired by recent studies aiming at devising semi-automatic procedures to speed-up the design of cutting guides, the present paper aims to propose a new approach to the design, and production, of custom-made surgical guides to assist the sternal osteotomy for the correction of chest deformities (i.e. PA). The proposed framework entails both a series of automatic and user-guided tasks able to design the patient-tailored guide from medical imaging to the final AM prototype.

In fact, by developing a proper procedure integrating MI and 3D reconstruction methods (Uccheddu et al., 2018; Widmann et al., 2016) it is possible to retrieve the exact 3D geometry of the sternal body. On this geometry, it is then possible to design and produce a custom surgical guide to be positioned on the patient's chest, thus

ensuring a successful outcome of the intervention. Since one of the main aims is to assess the effectiveness of the proposed framework, this has been developed by using commercial software packages (i.e. 3D slicer and Geomagic Design X).

2. Materials and methods

The proposed procedure, which starts from the availability of CT images of the patient to be treated, consists of the following steps:

- i. Image processing and 3D medical model reconstruction
- ii. Virtual design of desired cut planes
- iii. Custom surgical guide design
- iv. Virtual simulation of the surgical intervention
- v. Manufacturing of the surgical guide.

The procedure has been developed with reference to a single case study i.e. a 16 years old man with a severe chondro-sternal malformation characterized by a significant accentuation of the normal curvature and by a widening of the distal portion of the sternum itself. The proposed method has been virtually validated by studying two more patients (male, 14 years old and female, 13 years old). All subjects have been informed of the nature of the experimentation and written consent was obtained. The Ethical Guidelines of both the University of Florence and Italian law have been respected while performing the experimentation.

2.1. Image processing and 3D medical model reconstruction

The 3D model reconstruction of the patient affected by the chest deformity begins with the acquisition of 3D volumetric

thorax images in which the anatomy of interest (i.e. the sternal body) has sufficient signal intensity and contrast—combined with minimal artefact—to be differentiated from surrounding structures. Most models are generated from CT or MRI; therefore, the quality of the model depends on the quality of the imaging source data. Thin reconstructed images can allow for accurate anatomy delineation, but usually require cumbersome post processing. Both cardiac movement and breathing artefacts challenge the accuracy of the subsequent model. 3D printing from CT images should be reconstructed ideally on the order of 1 mm in thickness. Because narrowly reconstructed images have lower signal, the use of smoother kernels that make image segmentation easier is often desirable (Ahmadi, Kangarani Farahani, Sotudeh, Zhaleh, & Garshasbi, 2013; Al-Ameen, Sulong, & Md Johar, 2013; Maini & Aggarwal, 2010).

Once the medical images are properly restored and noise is reduced (see for instance Fig. 3), it is possible to perform the image segmentation, namely, the delineation of the desired tissues (Abid Hasan & Ko, 2016; Olabarriaga & Smeulders, 2001; Pham, Xu, & Prince, 2000; Sharma et al., 2010).

This process allows discriminating between the anatomy of interest and the adjacent tissues. Several algorithms are available to perform image segmentation, ranging from manual to fully automated approaches tailored on the specific anatomy. The segmentation process is often semi-automated, combining an initial step of automated segmentation followed by manual corrections. The tissue boundaries can be identified on successive 2D images (see Fig. 4) that are subsequently linked to form a closed surface and stored in standard tessellation language (STL) format.

The chest CTs of the patient has been processed in an open-source environment named 3D Slicer (Fedorov et al., 2012). 3D Slicer is a free and open source software package for medical image



Fig. 3. CT scan results for the patient involved in experimentation.



Fig. 4. Segmentation examples on the CT scan depicted in Fig. 3.

computing (MIC) and visualization. Initially developed as Master's thesis project in 1999 at the Massachusetts Institute of Technology (MIT), it has been continuously developed and improved, also thanks to the financial support of the National Institutes of Health (NIH). The first step of the patient-specific approach entailed a denoising process, involving a Gauss blur filter and histogram stretching procedure applied to the CT volumetric data. The second step involves the segmentation of the thorax images based on the thresholding of the Hounsfield values, while the third step regards the 3D model calculation.

The 3D geometries of the sternal and chest bones have been created without applying smoothing filters after segmentation (see Fig. 5a). The obtained triangular mesh models have been, then, optimized by reducing the number of polygons, while keeping the level of details and resolution of the original model. Finally, the sternal bone has been isolated and the Stereolithographic (STL) model has been generated as shown in Fig. 5b.

2.2. Virtual design of desired cut planes

Once the 3D model of the patient sternum is available, it is possible to virtually plan the best position and the angle of the planes defining the V-shaped cut. The virtual simulation can be carried out by using one of the available Reverse Engineering software packages. In this work, Geomagic Design X software (<http://www.geomagic.com/en/products-landing-pages/designx>) has been used both for the mesh manipulation and for the design of the surgical guide model (see Section 2.3). Due to the complex geometry of the sternum, a few steps for aiding the definition of the cutting planes are required. First, the mirror plane (i.e. a

roughly symmetrical plane of the mesh) has been detected using the approach proposed in Di Angelo and Di Stefano (2013) and created (see Fig. 6a). Then, the polyline defined by the intersection between such a mirror plane and the sternum mesh is automatically created. As a result, the silhouette of the sternum in correspondence of the mirror plane is described by such a polyline (see Fig. 6b).

Finally, polyline vertices are used to determine the convex hull by using the well-known Graham Scan algorithm (Anderson, 1978) (see Fig. 7a). At this point, the user intervention is required in order to select the segment ℓ spanning from one side to the other of the main concavity of the section (see Fig. 7b). This step could also be automatized by considering that ℓ is usually the maximum length segment among the one composing the convex hull. However, further tests are necessary in order to confirm this assumption. The endpoints p_1 and p_2 of segment ℓ are, respectively, close to the xiphisternal junction to the manubrium junction. Such points can

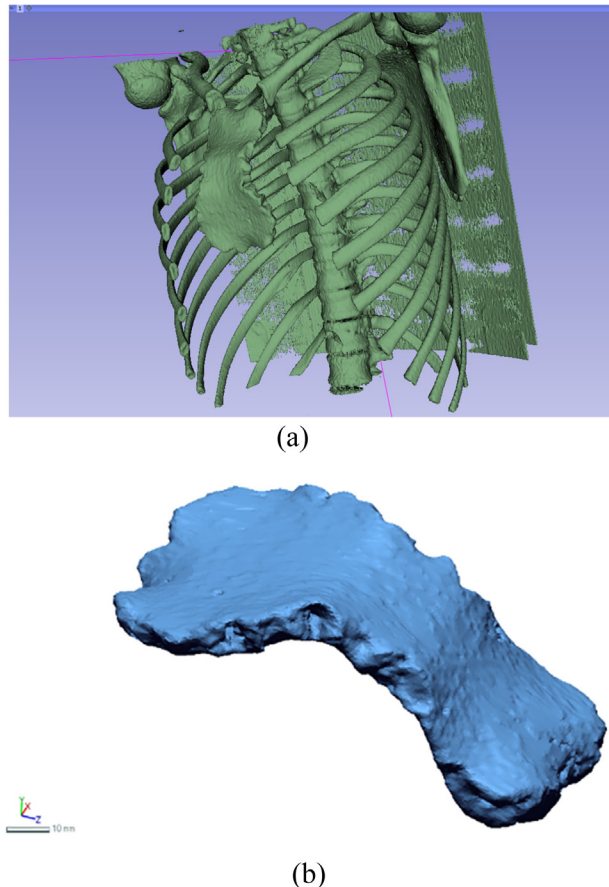


Fig. 5. (a) 3D geometry of the sternal and chest bones; (b) STL model of the sternum.

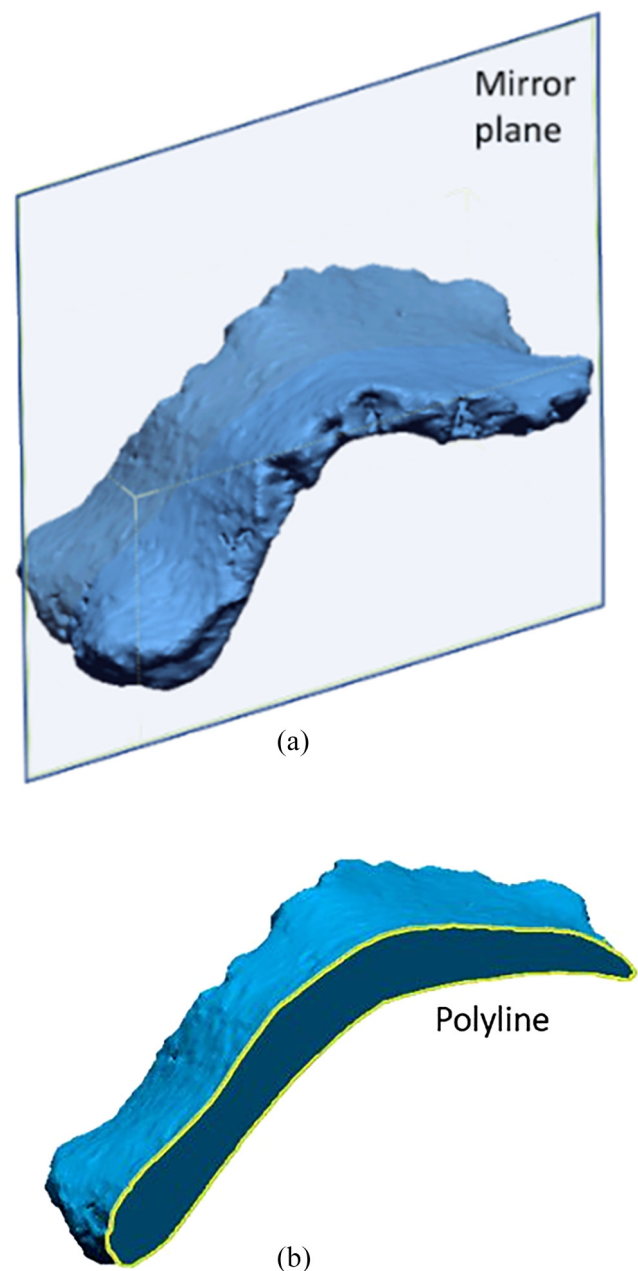


Fig. 6. (a) Detection of the mirror plane; (b) silhouette (polyline) of the sternum in correspondence of the mirror plane.

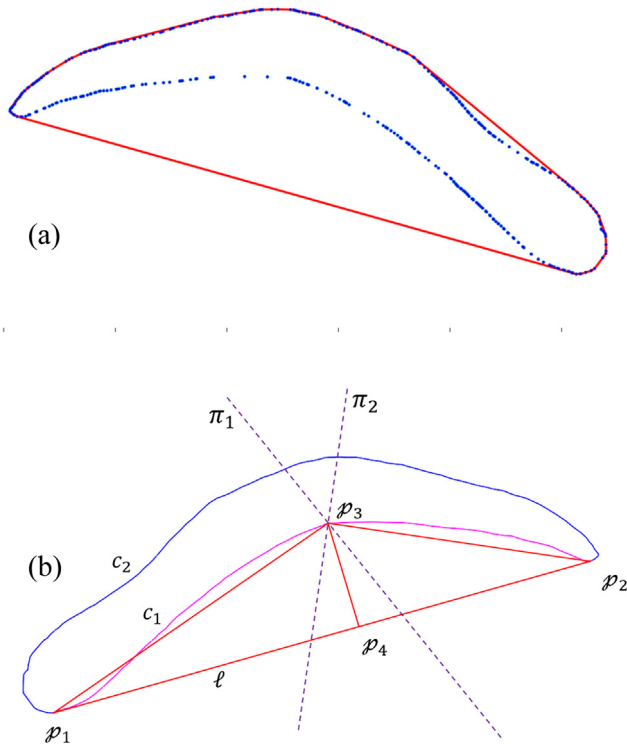


Fig. 7. (a) Convex hull of the silhouette of the sternum; (b) construction of parameters for determining the set of points (p_1, p_2, p_3) defining the vertices of a triangle used to derive the two cutting planes.

be used to split the curve μ into two curves μ_1 (magenta in Fig. 7b) and μ_2 (blue in Fig. 7b). A third point p_3 on μ_1 is selected as the one at the maximum distance from ℓ . This points set (p_1, p_2, p_3) defines the vertices of a triangle used to derive the two cutting planes, according to the assumption that $\overline{\mu_1 - \mu_3}$ and $\overline{\mu_2 - \mu_3}$ need to become aligned after the surgical intervention. The sought cutting planes π_1, π_2 are the ones orthogonal to the plane containing the polyline, passing by p_3 and orthogonal respectively to $\overline{\mu_1 - \mu_3}$ and $\overline{\mu_2 - \mu_3}$.

The planes π_1, π_2 have been used to virtually cut the sternum polygonal model, thereby obtaining two parts that have been subsequently rotated, around the axis orthogonal to the plane containing the polyline and passing by p_3 , by angles $\widehat{\mu_2 \mu_1 \mu_3}$ and $\widehat{\mu_1 \mu_2 \mu_3}$ respectively. Though the posterior cortex of the normomorph sternum is slightly arched, common medical practice suggests to overcompensate PA defect. Accordingly, the above-mentioned angles are selected to elide a prism allowing the sternum to be approximately flat (after the surgical intervention). Therefore, with reference to the case study, $\widehat{\mu_2 \mu_1 \mu_3} = 20^\circ$ and $\widehat{\mu_1 \mu_2 \mu_3} = 24^\circ$. In Fig. 8a, a representation of the sternum geometry and of the cutting planes is provided prior the PA surgical correction; in Fig. 8b the result of (virtual) surgical correction is depicted.

Since the proposed framework allows to test configurations different from traditional ones (i.e. the one commonly used in the surgical room), two additional virtual surgical corrections have been carried out by using lower cutting angles:

1. $\widehat{\mu_2 \mu_1 \mu_3} = 15.5^\circ$ and $\widehat{\mu_1 \mu_2 \mu_3} = 18.5^\circ$ ($\cong 77\%$ of the original cutting angle);
2. $\widehat{\mu_2 \mu_1 \mu_3} = 11^\circ$ and $\widehat{\mu_1 \mu_2 \mu_3} = 13^\circ$ ($\cong 55\%$ of the original cutting angle).

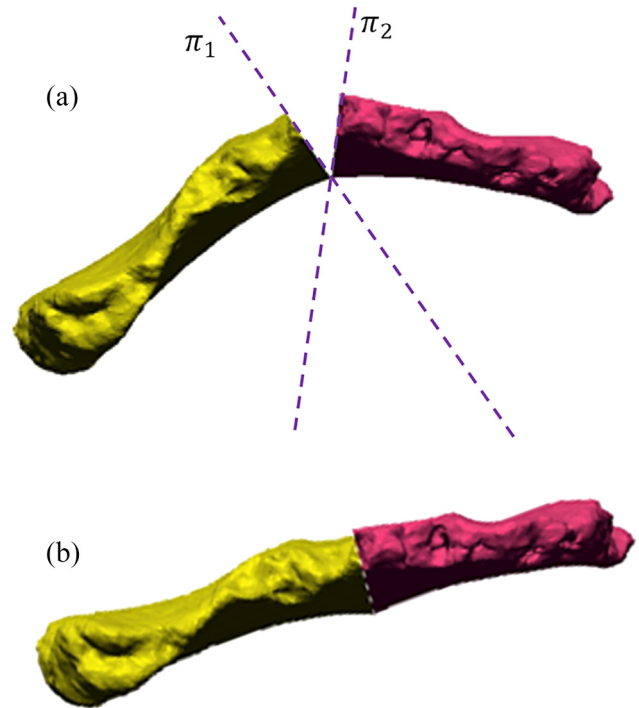


Fig. 8. (a) Representation of the sternum geometry and of the cutting planes prior the PA surgical correction; (b) virtual surgical correction.

In Fig. 9 the three alternatives (prior and after the virtual surgical correction) are compared.

To further validate the choice of the resection prism, the three configurations have been physically prototyped by using the Makerbot Replicator+, implementing the FDM technology (Parandoush & Lin, 2017) in order to preliminarily assess the surgical outcome. The selected material for manufacturing such prototypes is polylactic acid (PLA). In Fig. 10 the prototype model of the original solution ($\widehat{\mu_1 \mu_2 \mu_3} = 44^\circ$) is shown.

By comparing the results of the three different corrections, the original one has been selected as the most suitable. The procedure used so far has been developed on the assumption that the cut

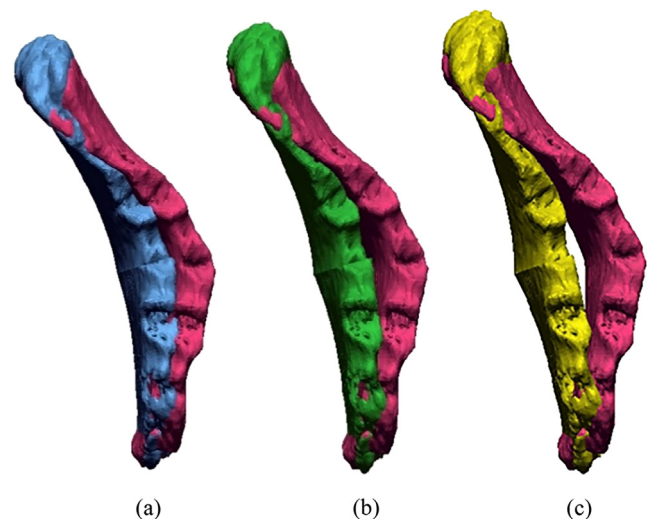


Fig. 9. Comparison between three alternatives with different cutting angles (prior and after the virtual surgical correction); (a) $\mu_2 \mu_1 \mu_3$; (b) $\mu_1 \mu_2 \mu_3$; (c) $\mu_1 \mu_2 \mu_3$.



Fig. 10. prototype of the sternum obtained using Makerbot Replicator+ starting from the model with cutting angles μ_1, μ_2, μ_3 .

needs to affects the entire sternum thickness. However, the sternum has a thin internal trabecular (spongy) body wrapped in two layers of cortical bone, the so-called anterior and posterior cortices. The posterior cortex fulfils the function of ultimate protection for the internal vital organs that are covered by the sternum, and therefore, as already mentioned, cannot be damaged for safety reasons. In order to make a constant depth cut possible, it is necessary to raise the edge of the resection prism by a value sufficient to guarantee the integrity of the posterior cortex. From a practical point of view, such a modification can be made by translating the intersection axis between the cutting planes π_1, π_2 along the direction defined by segment $\overline{\mu_3 - \mu_4}$ (see Fig. 7) thus obtaining two new planes π'_1 and π'_2 parallel to, respectively π_1 and π_2 . The intersection between such new planes defines a new axis whose intersection with the mirror plane is the point μ'_3 . By analysing

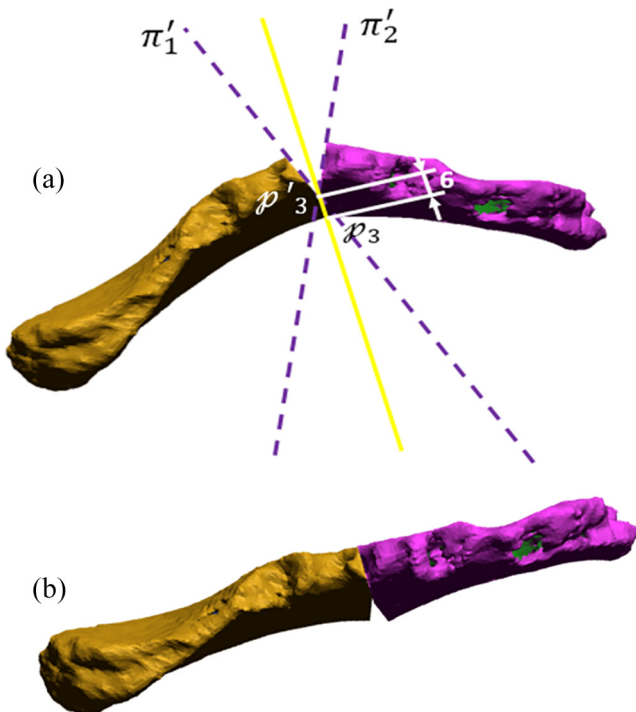


Fig. 11. (a) Intersection axis of the two cutting planes raised by six millimetres; (b) representation of the sternum geometry after the new surgical correction.

the CT images, it is possible to determine the best translational value (i.e. the distance $\mu_3 - \mu'_3$) for each patient; for safety reasons, such a value can be set equal to at least three times the thickness value of the posterior cortex. With reference to the case study, the intersection axis of the two cutting planes was raised by six millimetres as shown in Fig. 11a. In Fig. 11b, a representation of the sternum geometry after the new surgical correction is provided.

2.3. Custom surgical guide design

In order to ensure a quick and unambiguous positioning of the surgical guide on the sternum and, at the same time, to avoid misalignment, the interface between the guide and the sternum anterior cortex are required to be coincident. Since the geometry of the sternum is irregular, it has been first necessary to process the mesh of the anterior cortex to make it more regular and continuous, while respecting the main anatomical characteristics of the bone. Accordingly, such a mesh has been selected, isolated (see Fig. 12a) and processed using typical reverse engineering tools (e.g. hole filling, cleaning, smoothing and boundaries correction) so as to remove noise and defects (Fig. 12b). The processing has required several steps and a particular attention to the preservation of the main anatomical conformations of the sternal surface, mainly in the region of defect protrusion. A freeform surface \mathcal{S} , fitting the processed mesh, has then been modelled (see Fig. 12c);

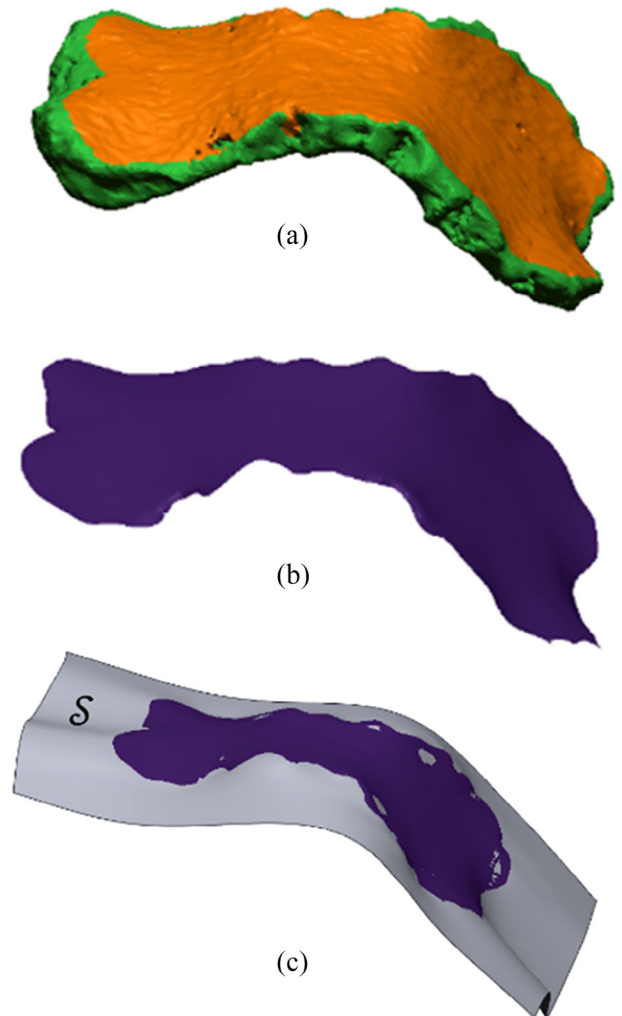


Fig. 12. (a) Segmented mesh for the extraction of the anterior cortex; (b) processed mesh of the anterior cortex; (c) freeform surface \mathcal{S} fitting the processed mesh.

this crucial step enabled to obtain a continuous surface used to design the lower part of the surgical guide (i.e. the guide surface in contact with the sternum) thus guaranteeing the correct coupling and positioning.

To model the shape of the surgical guide, it is necessary to define two new planes ξ_1 and ξ_2 perpendicular, respectively, to π'_1 and π'_2 , and positioned at a distance d from π'_3 (see Fig. 13a). Such a distance should be sufficient to properly drive the blade during the cutting phase. In particular, the blade should be driven for at least 10 mm before the cutting occurs. Since the thickness of the bone to be resected typically varies in the range 12–16 mm

Mahinda & Murty, 2009, a value $d = 20\text{--}25$ mm can be considered a good option, taking into account that as already stated in Section 2.2 the saw should not completely cut the sternum.

On planes ξ_1 and ξ_2 it is now possible to draft a 2D sketch representing the desired surgical guide contours. Eventually, these are projected on the surface \mathcal{S} and two 2D splines are used to close the contour (see Fig. 13b). The obtained closed contour is used to cut the surface \mathcal{S} so as to retrieve a basis surface resembling the desired shape of the cutting guide. By thickening the basis surface,

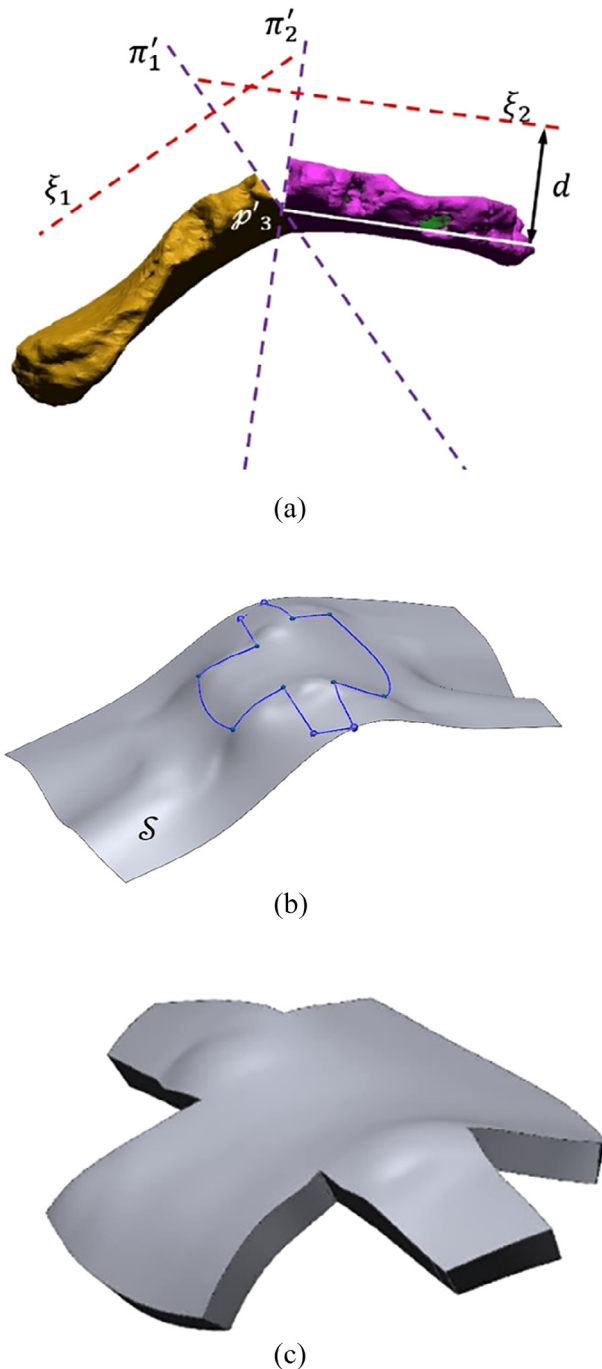


Fig. 13. (a) Definition of the two new planes ξ_1 and ξ_2 ; (b) closed contour obtained by projecting the 2D sketch drafted on the planes ξ_1 and ξ_2 on the surface \mathcal{S} ; (c) first-attempt of the surgical guide.

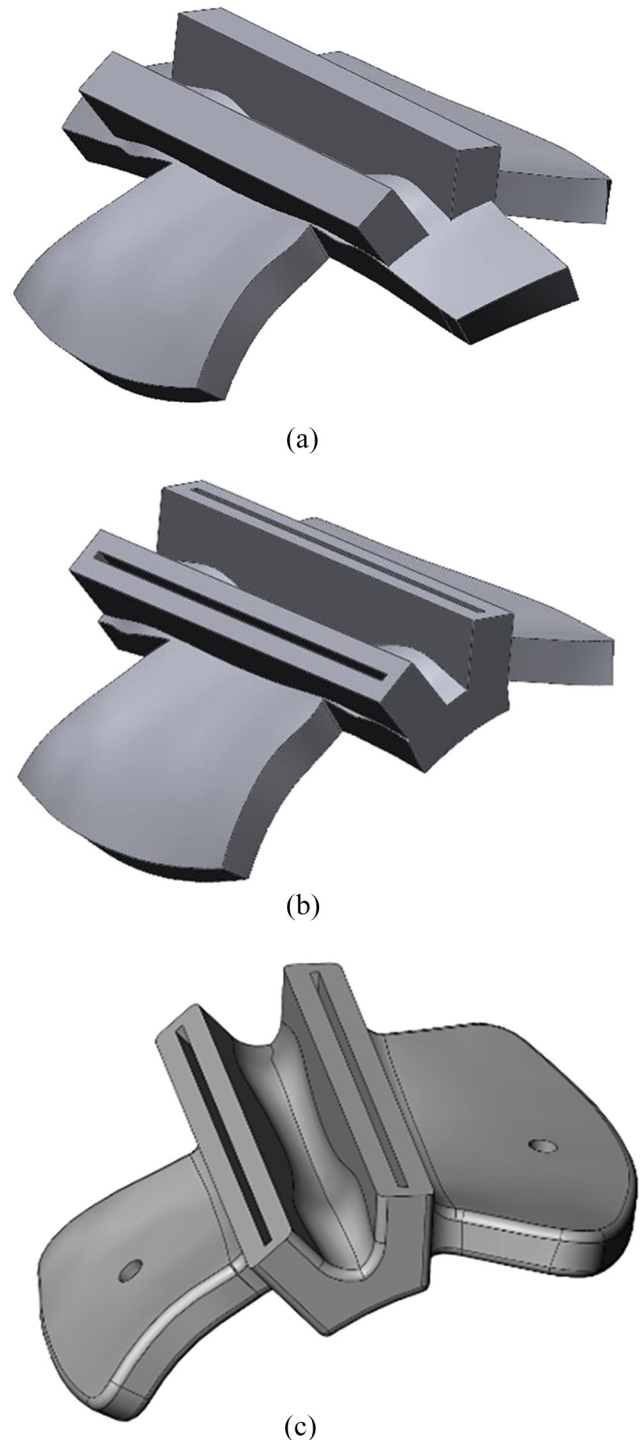


Fig. 14. (a) First-attempt guide with extruded rectangles; (b) removal of exceeding parts; (c) final 3D model of the surgical guide.

e.g. with a value equal to 5 mm, it is possible to design a first-attempt of the surgical guide (see Fig. 13c) to be further refined.

On planes ξ_1 and ξ_2 two rectangles are drafted. Their length has been decided by taking into account the necessity of operating on all the transversal area of the sternum; the width has been decided equal to six times the saw blade thickness. Such rectangles are extruded up to the upper surface of the first-attempt guide (see Fig. 14a). The exceeding parts are then discarded by the model and the slots for the saw blades are obtained by cut extruding a rectangular sketch (with width equal to the thickness of the blade) on both the extruded rectangles (see Fig. 14b). To lock the surgical guide on the sternum, two through holes of diameter 2.4 mm (to accommodate self-tapping screws) are eventually modelled; moreover, the part is filleted to improve its design. The overall result of the procedure described above is depicted in Fig. 14c and consists of the final 3D model of the cutting guide, ready to be manufactured.

To validate the effectiveness of the design, a first prototype of the surgical guide has been realized in PLA material by using the Makerbot Replicator+ 3D. The obtained prototype has been coupled with the sternum prototype to visually assess their coupling (see Fig. 15). Of course, PLA is not suitable for a surgical use; for this reason, it is necessary to study possible alternatives, as described in the Section 2.5.

2.4. Virtual simulation of the surgical intervention

Given the availability of patient sternum, surgical guide and surgeon instrument (oscillating saw) CAD models it is possible to virtually simulate the surgical intervention. As depicted in Fig. 16, several tasks can be simulated such as, for instance, the accessibility of the blade into the guide, the correct penetration of the blades, the expected final positioning of the sternum downstream the sternum cut.

2.5. Manufacturing of the surgical guide

Although not implantable, the cutting template is supposed to come into contact with biological tissues and fluids; for this reason, the chosen material must fulfill the biocompatibility requirement and, at the same time, must resist to the mandatory sterilization cycles (Espalin et al., 2009). The more common medical instrumentations sterilization techniques are the autoclave, the ethylene oxide exposure, the hydrogen peroxide and the gamma radiations (Rogers, 2017). The most common method adopted at Meyer Children Hospital is the first one where water is boiled under pressure, creating saturated steam, which condenses on the object to be sterilized. To guarantee a uniform temperature distribution of the



Fig. 15. Prototype of the surgical guide obtained using Makerbot Replicator+ 3D.

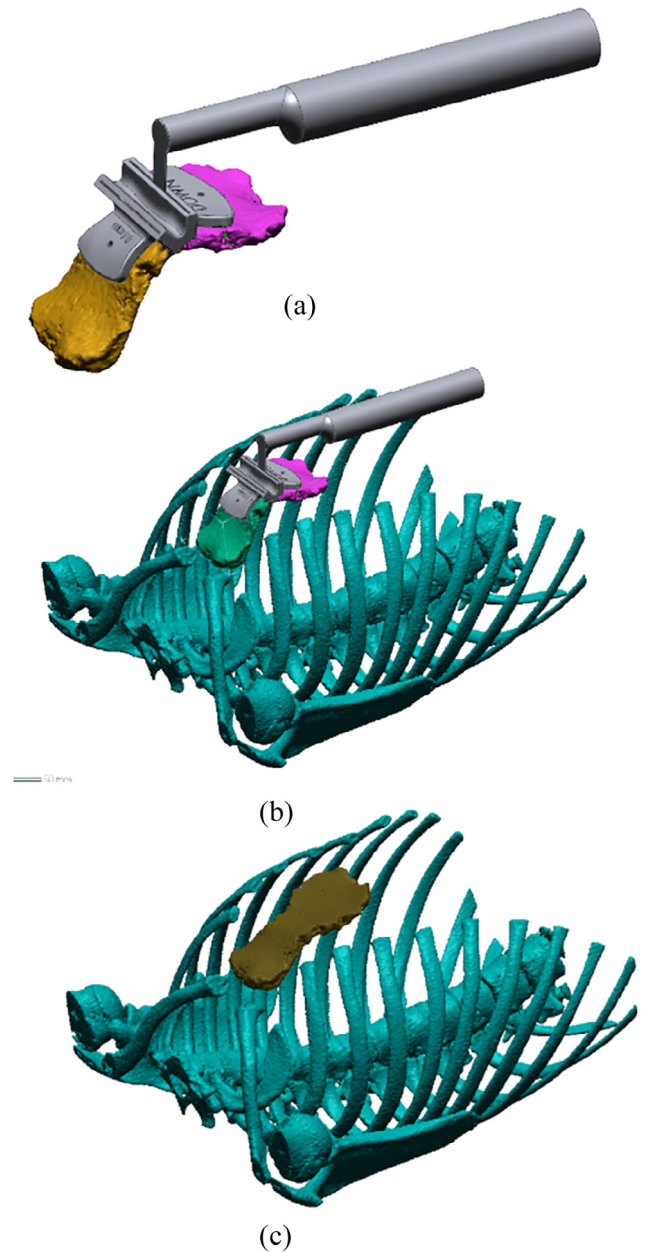


Fig. 16. (a) Virtual simulation of the blade accessibility into the surgical guide; (b) Virtual simulation of the mutual positioning between the chest and the surgical guide and of the guide with the saw; (c) Virtual simulation of restored sternum after the virtual surgery intervention.

steam, the process is performed in a vacuum environment. The sterilization standard for the surgical room is 20 min at 121 °C under a 2 bar pressure.

Most FDM Plastic materials are extruded at temperatures well above the 121 °C recommended for steam sterilization (Fedorovich, Alblas, Hennink, Öner, & Dhert, 2011). However, autoclaving often compromises the structural integrity of many plastics as reported in Meseguer-Olmo et al. (2013), Rozema et al. (1991). Therefore, to manufacture the surgical guide a scouting of suitable materials has been carried out.

The available plastic materials are many: ABSi, ABS-M30, ABS-M30i, ABS-ESD7 and PC-ABS, ABS derivatives, PC plastics, PC-ISO, PPSF, the FDM Nylon 6, 12 and 12 CF technical plastics, and the thermoplastic resins ULTEM™ 9085 and ULTEM 1010. Due to its excellent resistance, thermal stability and its resistance to autoclave sterilization steam temperatures (Perez et al., 2012), the

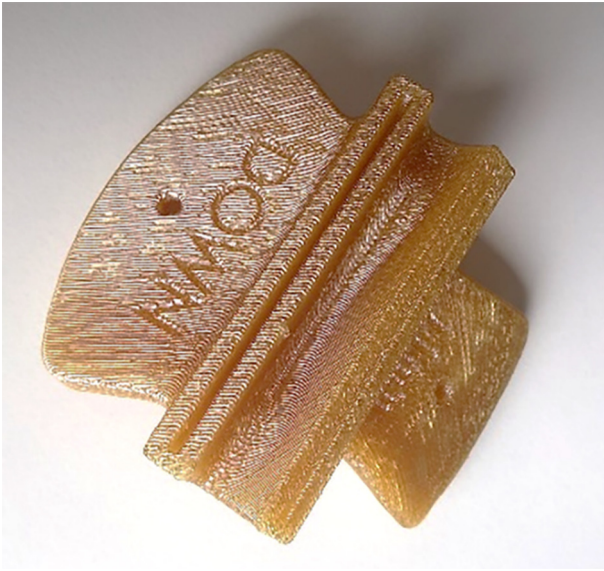


Fig. 17. Surgical guide produced using the Fortus 450mc 3D printer; the selected material to create the guide is ULTEM 1010 thermoplastic resin.

ULTEM 1010 thermoplastic resin was selected as the best option for the surgical guide fabrication. Using such a material the guide has been produced by means of a Fortus 450mc, implementing FDM (Velasco, Lancheros, & Garzón-Alvarado, 2016) technology (see Fig. 17).

3. Discussion and conclusions

A novel approach to design and manufacture, by using additive manufacturing techniques, patient-tailored surgical guides capable to assist the sternal osteotomy for the correction of Pectus Arcuatum, has been proposed in this paper.

The proposed approach entails a semi-automatic procedure starting from medical images representing the thorax of the patient (CT/MRI scans). First, a 3D reconstruction of the actual patient sternal body is carried out; next, a virtual design of the desired shape of the sternum (i.e. the geometry of the sternal body after the intervention) is performed. Such a virtual geometry is, then, used to decide the correct angles for the bone cutting and to design the patient-specific surgical guide. Finally, the surgical guide can be produced using AM and can be prepared for its use during the intervention. The proposed procedure has been developed with reference to a single case study. When compared to traditional intervention, the proposed procedure promises to allow a more precise preoperative planning: before entering the surgical room, the surgeon knows the exact patient's anatomy and each step of the surgical procedure. Moreover, the availability of a personalized surgical guide could allow both to optimize (e.g. changing the choice of the best surgical technique for the patient) and to guide the surgical act (reproducing the preoperative planning and improving of the accuracy).

As already mentioned, to test its effectiveness two additional case studies (male, 14 years old and female, 13 years old) have been investigated. Also for these validation cases automatic tasks such as the identification of the mirror plane and the definition of the cut planes have been correctly obtained and user-guided steps (carried out by a skilled CAD user) have been performed following the same identical tasks. Accordingly, this work proves to be a significant step towards an automatic design of patient specific cutting guides to assist sternal osteotomies. The proposed framework has been developed by using commercial software

packages (i.e. 3D slicer and Geomagic Design X); future works will be addressed to the development of a completely automatic procedure to retrieve the guide 3D model to be processed with AM and an appositely devised software to be easily used by medical staff will be developed. Moreover, since the designed guides are ready to be used in surgery room, a medical assessment of such a device will be performed as soon as the three patients will undergo surgical intervention.

Acknowledgments

The authors wish to acknowledge the valuable contribution of Marta Romagnoli in providing useful hints for processing 3D data. The authors also wish to thank the Fondazione Ospedale Pediatrico Meyer Onlus (<http://www.fondazionemeyer.it/>) for funding the T3DDY lab (Personalized paediatrics by inTegrating 3D aDvanced technology), which originated and made possible this research.

References

- Abid Hasan, S. M., & Ko, K. (2016). Depth edge detection by image-based smoothing and morphological operations. *Journal of Computational Design and Engineering*, 3(3), 191–197.
- Ahmadi, R., Kangarani Farahani, J., Sotudeh, F., Zhaleh, A., & Garshasbi, S. (2013). Survey of image denoising techniques. *Life Science Journal*, 10(1), 753–755.
- Al-Ameen, Z., Sulong, G., & Md Johar, M. G. (2013). Employing a suitable contrast enhancement technique as a pre-restoration adjustment phase for computed tomography medical images. *International Journal of Bio-Science and Bio-Technology*, 5(1).
- Anderson, K. R. (1978). A reevaluation of an efficient algorithm for determining the convex hull of a finite planar set. *Information Processing Letters*, 7(1), 53–55.
- Carfagni, M., Furferi, R., Governi, L., Servi, M., Uccheddu, F., Volpe, Y., & McGreevy, K. (2017). Fast and low cost acquisition and reconstruction system for human hand-wrist-arm anatomy. In *Procedia Manufacturing*, 2351–9789, 11, 1600–1608.
- Chen, X., Xu, L., Yang, Y., & Egger, J. (2016). A semi-automatic computer-aided method for surgical template design. *Scientific Reports*, 6, 20280.
- Di Angelo, L., & Di Stefano, P. (2013). Bilateral symmetry estimation of human face. *International Journal on Interactive Design and Manufacturing*, 7(4), 217–225.
- Espalín, D., Arcaute, K., Rodriguez, D., Medina, F., Posner, M., Wicker, R. (2009). Fused deposition modeling of polymethylmethacrylate for use in patient-specific reconstructive surgery. In *20th Annual international solid freeform fabrication symposium, SFF 2009* (pp. 569–583).
- Farré-Guasch, E., Wolff, J., Helder, M. N., Schulten, E. A. J. M., Forouzanfar, T., & Klein-Nulend, J. (2015). Application of additive manufacturing in oral and maxillofacial surgery. *Journal of Oral and Maxillofacial Surgery*, 73(12), 2408–2418.
- Fedorov, A., Beichel, R., Kalpathy-Cramer, J., Finet, J., Fillion-Robin, J.-C., Pujol, S., ... Kikinis, R. (2012). 3D Slicer as an image computing platform for the Quantitative Imaging Network. *Magnetic Resonance Imaging*, 30(9), 1323–1341.
- Fedorovich, N. E., Alblas, J., Hennink, W. E., Öner, F. C., & Dhert, W. J. A. (2011). Organ printing: The future of bone regeneration? *Trends in Biotechnology*, 29(12), 601–606.
- Fokin, A. A., Steuerwald, N. M., Ahrens, W. A., & Allen, K. E. (2009). Anatomical, histologic, and genetic characteristics of congenital chest wall deformities. In *Seminars in thoracic and cardiovascular surgery* (Vol. 21, No. 1, pp. 44–57). WB Saunders.
- Fonkalsrud, E. W., & Anselmo, D. M. (2004). Less extensive techniques for repair of pectus carinatum: The undertreated chest deformity. *Journal of the American College of Surgeons*, 198(6), 898–905.
- Goodfellow, J., & O'Connor, J. (1978). The mechanics of the knee and prosthesis design. *Journal of Bone and Joint Surgery - Series B*, 60 B(3), 358–369.
- Jeune, M., Carron, R., Beraud, C., & Loaec, Y. (1954). Polychondrodystrophie avec blocage thoracique d'évolution fatale. *Pediatric*, 9(4), 390–392.
- Kim, S. Y., Park, S., Kim, E. R., Park, I. K., Kim, Y. T., & Kang, C. H. (2016). A case of successful surgical repair for pectus arcuatum using chondrosteronoplasty. *Korean Journal of Thoracic and Cardiovascular Surgery*, 49(3), 214–217.
- Mahinda, H. A. M., & Murty, O. P. (2009). Variability in thickness of human skull bones and sternum—An autopsy experience. *Journal of Forensic Medicine and Toxicology Year*, 26(2), 26–31.
- Martínez-Ferro, M., Fraire, C., & Bernard, S. (2008). Dynamic compression system for the correction of pectus carinatum. In *Seminars in pediatric surgery* (Vol. 17, No. 3, pp. 194–200). WB Saunders.
- Meseguer-Olmo, L., Vicente-Ortega, V., Alcaraz-Baños, M., Calvo-Guirado, J. L., Vallet-Regí, M., Arcos, D., & Baeza, A. (2013). In-vivo behavior of Si-hydroxyapatite/polycaprolactone/DMB scaffolds fabricated by 3D printing. *Journal of Biomedical Materials Research - Part A*, 101 A(7), 2038–2048.
- Olabarriaga, S. D., & Smeulders, A. W. M. (2001). Interaction in the segmentation of medical images: A survey. *Medical Image Analysis*, 5(2), 127–142.

- Parandoush, P., & Lin, D. (2017). A review on additive manufacturing of polymer-fiber composites. *Composite Structures*, 182, 36–53.
- Perez, M., Block, M., Espalin, D., Winker, R., Hoppe, T., Medina, F., & Wicker, R. (2012). Sterilization of FDM-manufactured parts. In *23rd Annual international solid freeform fabrication symposium - an additive manufacturing conference, SFF 2012* (pp. 285–296).
- Pham, D. L., Xu, C., & Prince, J. L. (2000). Current methods in medical image segmentation. *Annual Review of Biomedical Engineering*, 2(2000), 315–337.
- Preethi, S. J., & Rajeswari, K. (2010). Image enhancement techniques for improving the quality of colour and gray scale medical images. *International Journal on Computer Science and Engineering*, 1, 18–23.
- Maini, R., & Aggarwal, H.. A comprehensive review of image enhancement techniques. *Journal of Computing*, 2(3), 8–13.
- Rogers, S. O. (2017). Surgical perspective: Centers for disease control and prevention guideline for the prevention of surgical site infection 2017. *Surgical Infections*, 18(4), 383–384.
- Rozema, F. R., Bos, R. R. M., Boering, G., van Asten, J. A. A. M., Nijenhuis, A. J., & Pennings, A. J. (1991). Effects of different steam-sterilization programs on material properties of poly(L-lactide). *Journal of Applied Biomaterials*, 2(1), 23–28.
- Sharma, N., Ray, A. K., Shukla, K. K., Sharma, S., Pradhan, S., Srivastva, A., & Aggarwal, L. (2010). Automated medical image segmentation techniques. *Journal of Medical Physics*, 35(1), 3–14.
- Uccheddu, F., Carfagni, M., Governi, L., Furferi, R., Volpe, Y., & Nocerino, E. (2018). 3D printing of cardiac structures from medical images: an overview of methods and interactive tools. *International Journal on Interactive Design and Manufacturing*, 12(2), 597–609.
- Velasco, M. A., Lancheros, Y., & Garzón-Alvarado, D. A. (2016). Geometric and mechanical properties evaluation of scaffolds for bone tissue applications designing by a reaction-diffusion models and manufactured with a material jetting system. *Journal of Computational Design and Engineering*, 3(4), 385–397.
- Widmann, G., Fischer, B., Berggren, J. P. M., Denhardt, A., Schullian, P., Reto, B., & Puelacher, W. (2016). Cone beam computed tomography vs multislice computed tomography in computer-aided design/computer-assisted manufacture guided implant surgery based on three-dimensional optical scanning and stereolithographic guides: Does image modality matter? *International Journal of Oral and Maxillofacial Implants*, 31(3), 527–533.
- Yao, X., Moon, S. K., & Bi, G. (2017). Multidisciplinary design optimization to identify additive manufacturing resources in customized product development. *Journal of Computational Design and Engineering*, 4(2), 131–142.